Online beam monitoring in the treatment of ocular pathologies at the INFN Laboratori Nazionali del Sud-Catania.

N. Givehchi[a,b], F. Marchetto[a], L.M. Valastro[c], A. Attili[a], M. A. Garella[a], S. Giordanengo[a], J. Pardo Montero[a], A. Boriano[a,b,d], F. Bourhaleb[b], R. Cirio[a,b], A. La Rosa[a,b], A. Pecka[a,b], C. Peroni[a,b], G. A. P. Cirrone[e], G. Cuttone[e], M. Donetti[a,f], S. Iliescu[a,b,g], S. Pittera[h], L. Raffaele[i]

[a] *INFN Sezione di Torino, Torino, Italy*

[b] *Dipartimento di Fisica Sperimentale, Università di Torino, Torino, Italy*

[c] *Azienda Ospedaliero-Universitaria Policlinico, Catania , Italy*

[d] *Azienda Sanitaria Ospedaliera S. Croce e Carle, Cuneo, Italy*

[e] *Laboratori Nazionali del Sud, INFN, Catania, Italy*

[f] *Fondazione CNAO ,Milano, Italy*

[g] *Istituto per la Ricerca e la Cura del Cancro (IRCC), Candiolo, Italy*

[h] *Centro Siciliano di Fisica Nucleare e Struttura della Materia (C.S.F.N.S.M.), Catania, Italy*

[i] *Azienda Ospedaliero-Universitaria Policlinico, Catania, Italy*

Abstract

A detector (MOPI) has been developed for the online monitoring of the beam at the Centro di AdroTerapia e Applicazioni Nucleari Avanzate (CATANA), where shallow tumours of the ocular region are treated with 62 MeV protons. At CATANA the beam is passively spread to match the tumour shape. The uniformity of the delivered

dose depends on beam geometrical quantities which are checked before each treatment. However, beam instabilities might develop during the irradiation affecting the dose distribution.

This paper reports on the use of the MOPI detector to measure the stability of the beam profile during the irradiation in the clinical practice. The results obtained in the treatment of 54 patients are also presented.

Key words: Online monitor, Quality Assurance, 2–D detectors, Proton Therapy

Introduction

Charged particle therapy with protons and heavier ions, known as hadron therapy, is gaining an increasing importance for the treatment of tumours. The main advantage with respect to the conventional radiation therapy with photons or electrons is that the ions passing through the tissue deposit most of the dose at a fixed depth, at the so called Bragg peak. The position in depth of the peak depends on the entrance energy of the ions. By properly adjusting the field size and the beam energy distribution, a proper conformation of the dose to the tumour volume can be achieved, while sparing at the same time the surrounding healthy tissues.

In the present clinical applications, different delivery techniques have been developed to achieve the most effective dose distribution. In the passive delivery systems a set of scatterers, collimators and absorbers are used to broaden and shape the beam to the tumour volume, while in the active delivery systems a uniform dose to the tumour is achieved by scanning the treatment volume with a narrow beam.

Dedicated detectors, based on multi-wire proportional chambers or planar ionization chambers, are used in the existing hadron therapy facilities to monitor dosimetric and geometrical beam parameters [1][2][3] on which the dose distribution depends. These detectors are designed to achieve a fine spatial segmentation and a limited thickness; furthermore, a fast response time is needed to detect any beam instability during the treatment.

The Centro di AdroTerapia e Applicazioni Nucleari Avanzate (CATANA) [7] is a italian hadron therapy facility located at the Laboratori Nazionali del Sud (LNS) of the Istituto Nazionale di Fisica Nucleare (INFN). In this centre a 62 MeV proton beam, extracted from a superconducting cyclotron, has been used since year 2002 for the treatment of ocular pathologies. The dose is delivered in a passive mode and, in order to monitor the beam stability during the treatment, a detector, called MOPI, has been developed by the collaboration between CATANA and the INFN of Torino. The online beam monitoring is particularly important at CATANA as its cyclotron has not been optimized specifically for medical applications.

The MOPI detector is a planar ionization chamber with the anode plane split into narrow strips to measure the beam shape. A fast measurement of the time evolution of the beam profile is obtained with a custom designed front-end electronics based on the ASIC TERA chips [4]. Similar detectors have been developed by INFN for other hadron therapy centres as ICPO (Institut Curie-Centre de protonthérapie de Orsay, France) [5] and CNAO (Centro Nazionale di Adroterapia Oncologia, Pavia, Italy) [6].

In this paper a short description of the CATANA beam delivery system is first presented. Then, the characteristics of the MOPI detector are summarized and its performance during the clinical use as online beam monitor is reported for the treatment of 54 patients.

Methods and Materials

The CATANA beam delivery

At CATANA the 62 MeV proton beam is shaped by the passive delivery system shown in Fig.1; following the beam direction, it consists of a scattering device, a range modulator, a range shifter, a set of monitor chambers and at the end a set of collimators.

The scattering system is located at about 3 meters upstream of the isocentre and is designed to broaden the beam in order to provide a uniform lateral off-axis dose distribution at the tumour.

The range shifter (RS) and the range modulator (RM), placed downstream the scattering system, are used respectively to change and to modulate the beam energy such that the dose distribution has a spread-out Bragg peak (SOBP) longitudinally overlapped with the treatment volume. The RS consists of 17x17 cm^2 square polymethylmethacrylate (PMMA) slabs of different thicknesses which are combined to achieve a total thickness in the range between 0.5 and 18.0 mm in steps of

0.2 mm. The RM is a PMMA wheel rotating at a fast constant speed and split in several angular sectors of increasing thickness; protons crossing the largest (smallest) thickness match the proximal (distal) edge of the SOBP.

The on-line control of the dose delivered to the patient during the treatment is provided by a set of parallel plate ionization chambers located downstream of the RM.

Following the monitor chambers, a 370 mm long brass collimator with an internal diameter of 25 mm (reference collimator) is used to limit the beam angular spread. A further patient specific collimator, whose aperture matches the planned target volume as seen from the beam line, is inserted at the output of the reference collimator, at 83 mm from the isocentre.

A system based on laser sources, also shown in Fig.1, is used to provide the isocentre identification, for patient centring, and to control the shape of the irradiation field.

The MOPI detector, used for the online monitoring of the beam shape, is described in the following sections; it is positioned after the dose monitor chambers as pointed out in Fig.1.

Beam quality assurance at CATANA

At CATANA a quality assurance check is performed before each treatment by measuring the cross-beam profiles along two orthogonal line paths in air using a remotely controlled scanning device. A p-type silicon diode, placed downstream of the reference collimator at the isocentre, is moved in the vertical and horizontal directions in steps of 0.5 mm. The measurement is performed before the insertion of the RS and RM elements and without any patient specific collimator. Typical results are shown in Fig.2.

From each cross-profile, the beam quality parameters flatness and symmetry can be determined using a restricted region (reference region), corresponding to the full width at half maximum minus twice the lateral penumbra. In this study the lateral penumbra is the distance between the 20% and the 80% of the dose at the plateau. The flatness R_t is used to estimate the maximum percentage deviation from the average dose; following the conventional definition used in radiotherapy, it is given by

$$R_t = \left(\frac{D_{Max} - D_{Min}}{D_{Max} + D_{Min}} \right) * 100$$

where D_{Max} and D_{Min} are the maximum and minimum doses measured in the reference region, a negative sign being assigned to R_t if D_{Max} occurs on the left half-part.

The symmetry S_t is defined by considering the doses D_L and D_R measured in the two points situated symmetrically at the left and right side of the centre of the reference region, where the quantity $\left|1-\frac{D_R}{D_L}\right|$ reaches its maximum:

$$S_t = \left(\frac{D_R}{D_L}\right) * 100$$

At CATANA, the clinical tolerances imposed on these parameters before each treatment are | Rt| < 3% and | St – 100% | < 3%.

The MOPI detector

The MOPI detector consists of strip ionization chambers developed for the CATANA application by the INFN and used for the online control of the beam geometry. The details on the construction and characterization of MOPI have been reported in a previous publication [5] and are briefly summarized in the following.

The MOPI detector covers a sensitive area of 12.8 x 12.8 cm^2 and is divided in two chambers separated by a common cathode plane, as shown in Fig.3. The anode plane of each chamber is segmented in 256 strips, resulting in a pitch of 0.5 mm, oriented along the vertical and horizontal directions. The gas gap of each chamber is 6 mm wide, filled with air and polarized at 500 V. The total water equivalent thickness of the whole detector is 0.16 mm.

The front-end electronics uses the TERA ASIC chip [4] to integrate the input currents and translate them into counts. A single count corresponds to a fixed amount of collected charge (quantum charge) that in the current implementation has been set to 200 fC. The maximum counting frequency is 5 MHz corresponding to saturation at an input current of 1 μA for the selected quantum charge; the minimum detectable current is at the level of a few pA.

Appropriate calibration coefficients have been determined for each channel following the procedure described in [5] to account for non-uniformities in the gas gap and in the electronic gain.

The distributions of the charges measured during a typical clinical application are shown in Fig.4 as a function of the position; they represent the projections of the beam particle distribution

respectively on the horizontal (X) and vertical (Y) directions. The beam symmetry is evaluated by using the skewness Sk_x and Sk_y calculated from these projections, as follows:

$$Sk_x = \frac{\sum_i s_i \cdot (x_i - \mu_x)^3}{\sum_i s_i \cdot \sigma_x^3}$$

and similarly for the Y projection. In the above formula s_i is the charge measured from the i_{th} strip, x_i is the coordinate of the strip centre, μ_x and σ_x are the mean and the r.m.s. of the distribution. For a symmetric beam projection the expected value of the skewness is zero.
In order to be insensitive to asymmetries in the portion of the beam which is removed by the downstream collimation system, the skewness and all the related parameters are calculated using the restricted windows shown in Fig.4; these correspond to the 50 strips matching the 25 mm aperture of the reference collimator. Applying these limits, the skewness is sensitive not only to the beam symmetry but also to the position of the beam relative to the selected windows. A tiny vertical misalignment between the beam and the collimator aperture is seen in Fig.4. The uncertainty on the position of the windows, estimated to be ±0.5 mm, translates into an uncertainty of about ±0.01 on the values of the skewness; such uncertainty does not affect the skewness variations monitored by the detector during a treatment.

To determine the correlation between the skewness and the R_t and S_t parameters, the currents in the last pair of dipole magnets of the extraction line have been varied relative to their nominal values with the intent of modifying the shape of the beam. For each setting of the currents a scanning of the beam has been performed with the diode and, at the same time, the beam skewness values have been measured with the MOPI detector. The results are shown in Fig.5, each point corresponding to a different current setting. The two sets of measurements show a good degree of correlation, justifying the use of MOPI as a sensitive tool to monitor the stability of the flatness and symmetry during a treatment. From Fig.5 it can be figured out that a variation of the skewness of ±0.05 corresponds to a change in flatness and symmetry larger than the clinical tolerances.

A custom DAQ system, described in detail in [5], reads out and stores the output of the 2 x 256 strips, computes the skewness values and transmits the results to the CATANA Control Room. Furthermore, it checks if the values are within tolerance and, in case of anomalous values, triggers an interlock to stop the

irradiation. The detector is read out every 0.5 s; this time is large enough to collect a reasonable statistics, while keeping the dose integrated in this interval only at a few percent of the total delivered dose.

Results

The MOPI detector has been added to the CATANA beam delivery and routinely used during treatments starting from 2006. Every morning the beam quality was certified by a measurement of the beam flatness and symmetry at the isocentre with the diode, as described in the previous sections. The MOPI detector was used for the online check of the stability of the beam skewness during subsequent treatment fractions. This section presents the skewness distributions obtained during a typical treatment fraction as well as the statistics collected during the first 54 treatments, each treatment consisting of four fractions delivered in consecutive days with the same set of passive elements.

Fig. 6 shows the skewness of the horizontal beam projection as a function of the acquisition time for a typical treatment fraction; the corresponding skewness distribution is presented in Fig.7. The main reason for a mean value deviating from zero is the beam projection not being perfectly centred relative to the window used in the calculation. For this treatment the skewness distribution has a RMS of 0.0011 and covers a full range of 0.006, smaller than the maximum deviation imposed by the clinical tolerances. Beam instabilities contribute to part of the observed fluctuations in Fig.6. In fact, the horizontal skewness appears to be correlated with the beam intensity as shown in Fig.8, where the skewness is now plotted as a function of the sum of the charges measured by the vertical strips. The dispersion of values at fixed intensity is consistent with the expected statistical fluctuations of the measurements.
The two beam projections corresponding to the maximum and minimum skewness of Fig.6, differing by 0.006, are compared in Fig.9(a). The ratio of the two distributions normalized to the same area is shown in Fig. 9(b). In the restricted window used for the skewness calculation and corresponding to the acceptance of the reference collimator, the two shapes differ at most by 1%.

It is interesting to compare how the skewness depends on the choice of the passive elements and how it varies between different fractions of the same treatment.

The skewness values averaged over the fractions are shown in figures 10 and 11 as a function of the thickness of the range shifter (RS) adopted for each specific treatment. Different symbols refer to different range modulators. The horizontal skewness appears to be centred at zero, independently of the RS thickness, and limited in the range ±0.04. The fluctuation tends to decrease as the RS thickness increases, an effect consistent with more scattering elements causing the beam to become broader and flatter. The same effect as a function of the RS thickness is also observed for the vertical skewness. However, a clear trend is observed, the vertical skewness deviating from zero at small thickness. This deviation is caused by the vertical beam projection not being perfectly aligned with the collimator acceptance window (see figure 4(b)); the broadening of the beam with the increase of the RS thickness mitigates the effect of this misalignment.

The day by day fluctuation of the beam shape has been evaluated by studying the distribution of the difference $Sk_i - \langle Sk \rangle$, where Sk_i is the average skewness for a single fraction and $\langle Sk \rangle$ is the skewness averaged over all the fractions for a single patient. The distribution, shown in Fig.12, includes both vertical and horizontal values for all the 54 treatments considered in this study; the RMS is 0.0046 and the maximum skewness variation over the fractions of a single treatment is within ±0.02. The day by day fluctuations appear though to be larger than the skewness fluctuations within a single fraction, but still within the maximum acceptable deviation discussed above.

Conclusions

An online beam monitor system, based on strip ionization chambers, has been developed for the CATANA proton therapy facility and is currently used to measure the horizontal and vertical beam projections during the treatments. The beam alignment and asymmetry is evaluated by calculating the horizontal and the vertical skewness in a restricted window corresponding to the aperture of the final reference collimator. It is shown in this paper that this quantity is strongly correlated with the beam parameters used for the beam quality assurance and can thus be used to monitor the beam stability during the treatment and to provide a fast error signal if it is found outside a tolerance limit.

This paper also reports the skewness measured in the clinical practice during the treatment of 54 patients, each treatment consisting of 4 fractions delivered in consecutive days. For a given treatment, a dependence on the choice of the passive elements is observed. The fluctuations of the skewness between different fractions of the same treatment, as well as the variations within a single fraction are typically within the tolerances. Any deviation of the skewness from the allowed

range provides a warning message to the CATANA control room without stopping the beam, although the hardware is ready to provide a fast interlock for the beam dump.

[1] Kraft G., “Tumor therapy with heavy charged particles”, Prog. Part. Nucl. Phys. 2000: 45; 473-544 and references therein.

[2] Pedroni E, Bacher R, Blattmann H, Bohringer T, Coray A, Lomax A, Lin S, Munkel G, Scheib S, Schneider U, Tourovsky A., “The 200-MeV proton therapy project at the Paul Scherrer Institute: Conceptual design and practical realization”, Med. Phys. 1995: 22; 37-53.

[3] Coutrakon G, Bauman M, Lesyna D, Miller D, Nusbaum J, Slater J, Johanning J, Miranda J., “A prototype beam delivery system for the proton medical accelerator at Loma Linda”, Med. Phys. 1991: 18; 1093-1099.

[4] Mazza G, Cirio R, Donetti M, La Rosa A, Luparia A, Marchetto F, Peroni C., “A 64-channel wide dynamic range charge measurement ASIC for strip and pixel ionization detectors”, IEEE Trans. Nucl. Sci. 2005: 52; 847-853.

[5] La Rosa A, Garella MA, Bourhaleb F, Cirio R, Donetti M, Giordanengo S, Givehchi N, Marchetto F, Martin F, Meyroneinc S, Peroni C, Pittà G., “A pixel ionization chamber used as beam monitor at the Institut Curie - Centre de Protontherapie de Orsay (CPO)”, Nucl. Instr. and Meth A. 2006: 565; 833-840.

[6] S. Giordanengo et al “The CNAO system to monitor and control hadron beams for therapy”, IEEE Dresden, Germany 19-25 October 2008 - Nuclear Science Symposium - Conference Record.

[7] Cirrone GAP, Cuttone G, Lojacono PA, Lo Nigro S, Mongelli V, Patti IV, Privitera G, Raffaele L, Rifuggiato D, Sabini MG, Salamone V, Spatola C, Valastro LM., “A 62 MeV proton beam for the treatment of ocular melanoma at Laboratori Nazionali del Sud-INFN”, IEEE Trans. Nucl. Sci. 2004: 51; No. 3, 860 – 865.

[8] Givehchi N, Marchetto F, Boriano A, Attili A, Bourhaleb F, Cirio R, Cirrone GAP, Cuttone G, Di Rosa F, Donetti M, Garella MA, Giordanengo S, Iliescu S, La Rosa A, Lojacono PA, Nicotra P, Peroni C, Pecka A, Pittà G, Raffaele L, Russo G, Sabini MG, Valastro LM., “Online monitor detector for the protontherapy beam at the INFN Laboratori Nazionali del Sud-Catania”, Nucl. Instr. and Meth A. 2007: 572; 1094-1101.

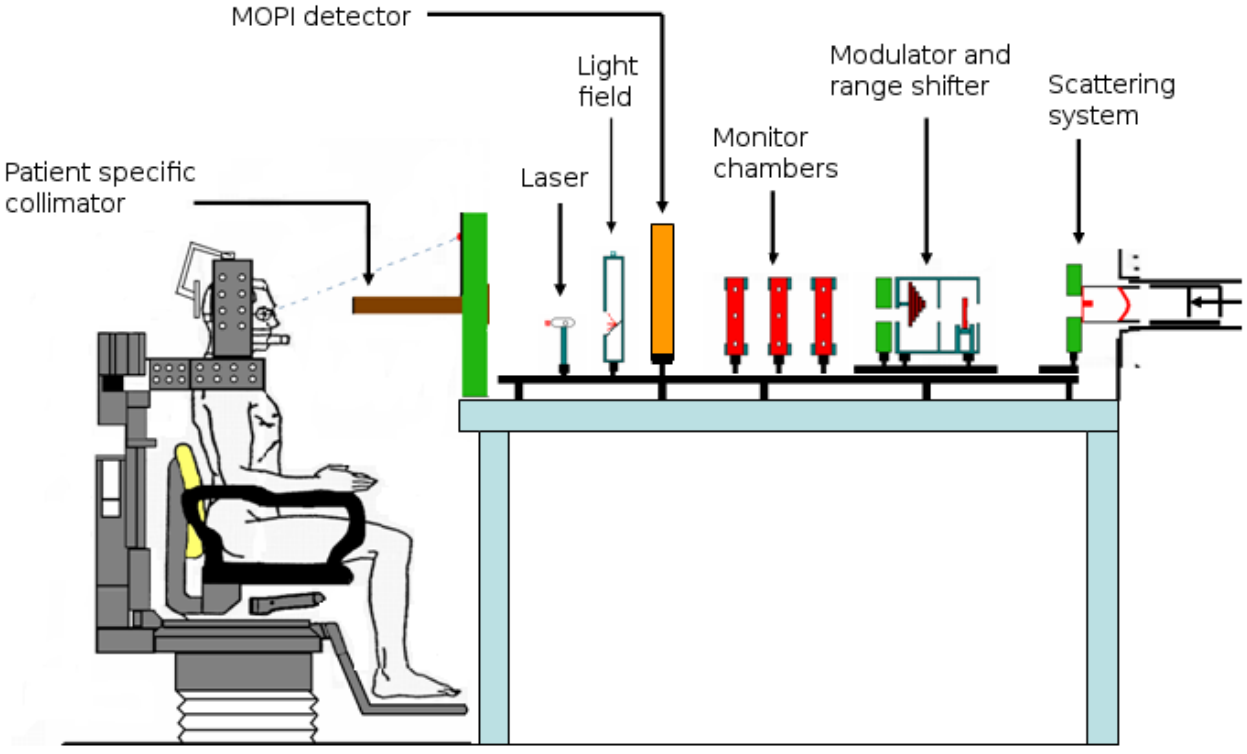

FIG. 1. Layout of the CATANA beam delivery system.

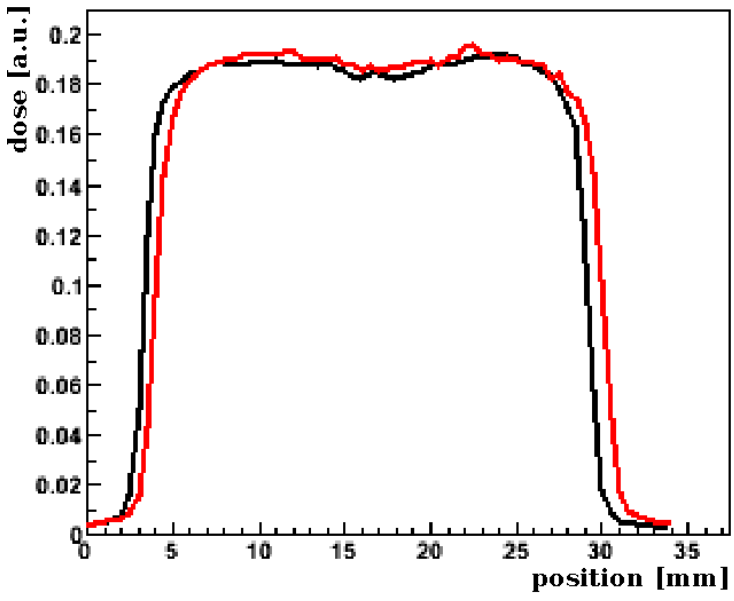

FIG. 2. Cross-beam profiles along the horizontal and vertical direction as measured with the diode in a pre-treatment beam quality assurance check.

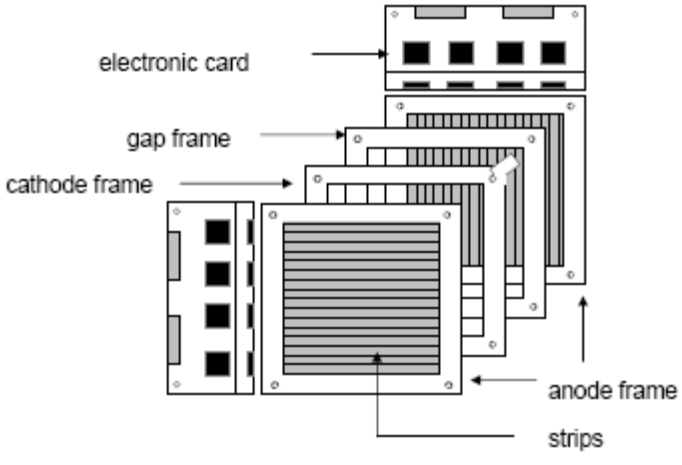

FIG. 3. Exploded view of the MOPI detector.

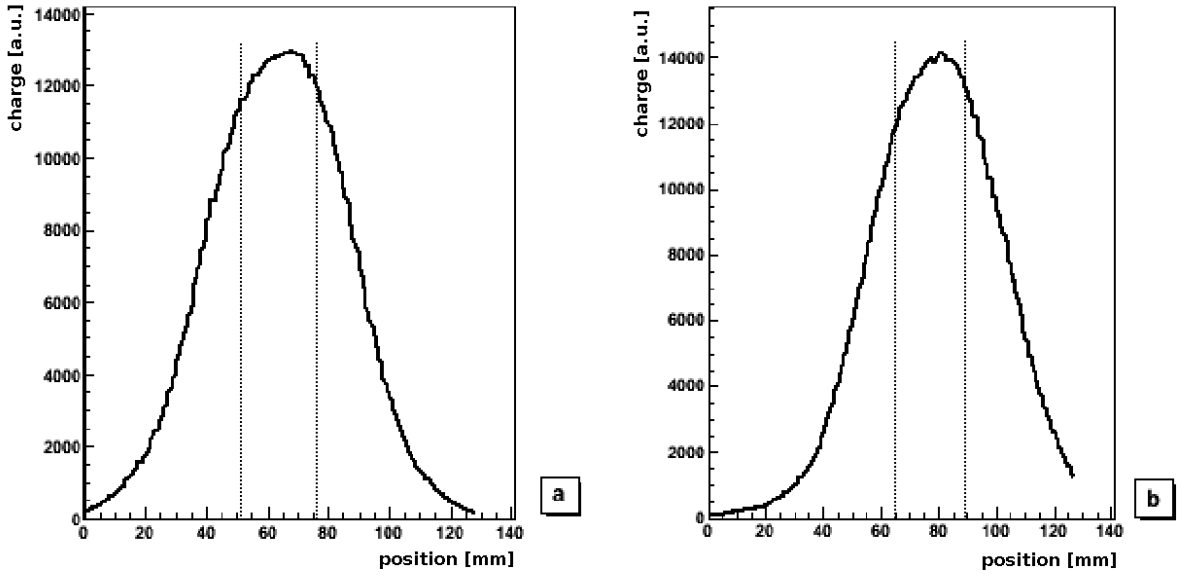

FIG. 4. Horizontal (a) and vertical (b) beam projections as measured with MOPI during a typical treatment. The region enclosed between the two vertical lines corresponds to the 50 strips matching the aperture of the reference collimator, from strip 103 to 152 in (a), and from strip 130 to 179 in (b).

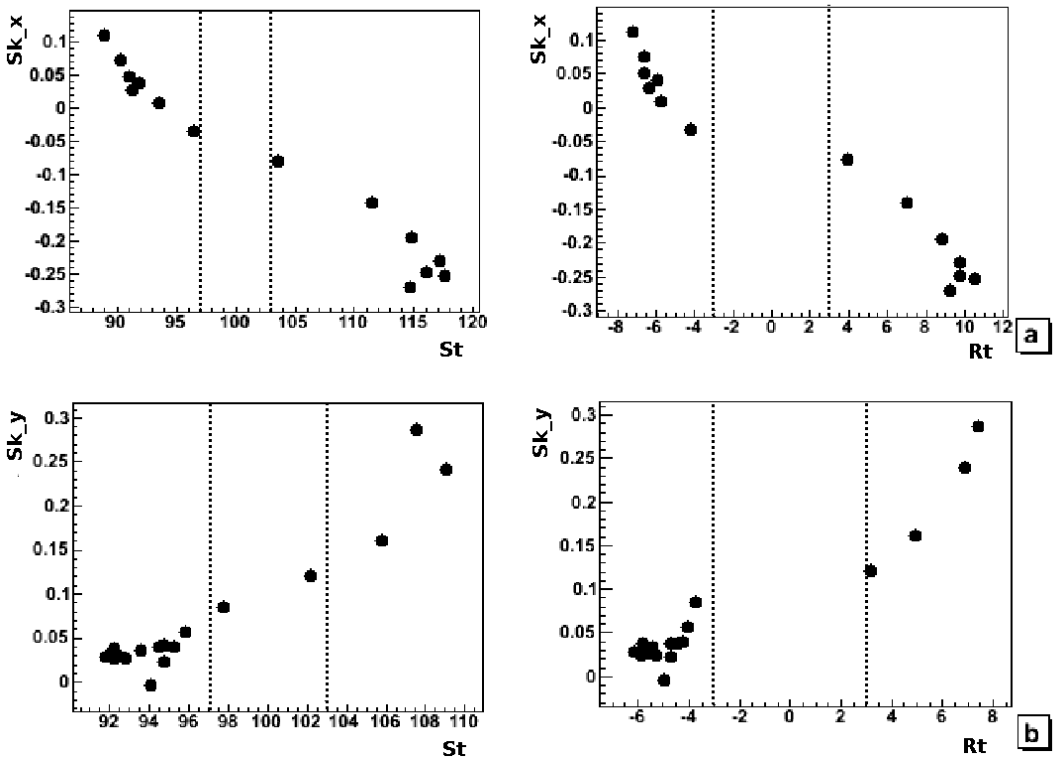

FIG. 5. Skewness vs. S_t and R_t in horizontal (a) and vertical (b) directions. The different points have been obtained by changing the currents of the last pair of dipole magnets around their nominal values. The bands correspond to the clinical tolerances on S_t and R_t.

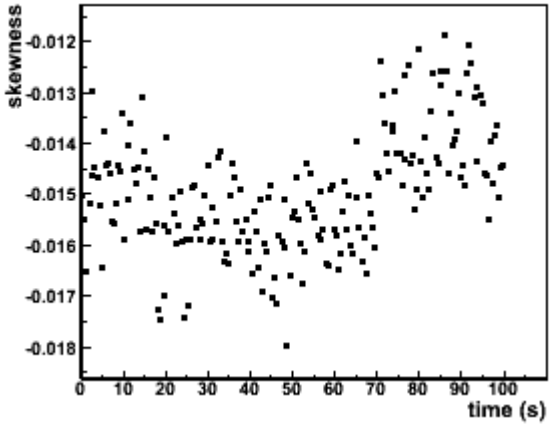

FIG. 6. Skewness of the horizontal beam projection measured with MOPI as a function of time in a typical treatment fraction.

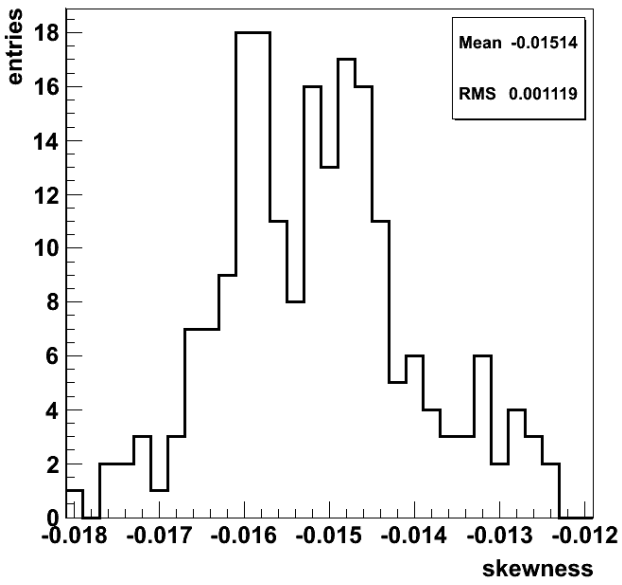

FIG. 7. Distribution of the skewness as measured in each time slot of Fig. 6.

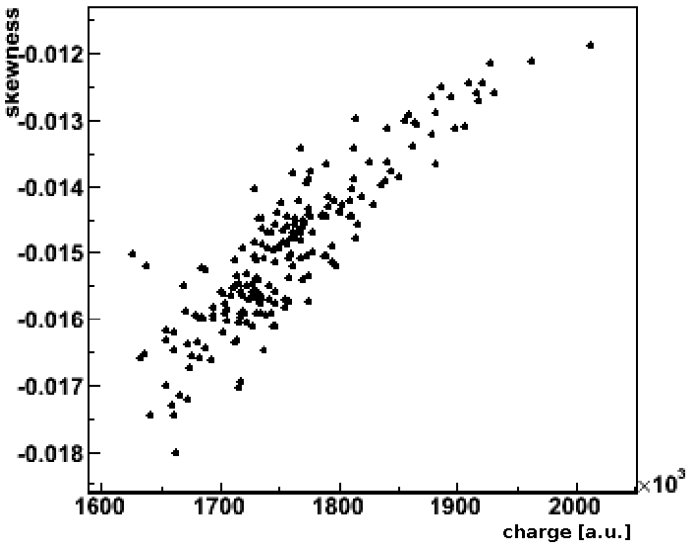

FIG. 8. Skewness as a function of the total measured charge for the same treatment of Fig. 6 and Fig.7.

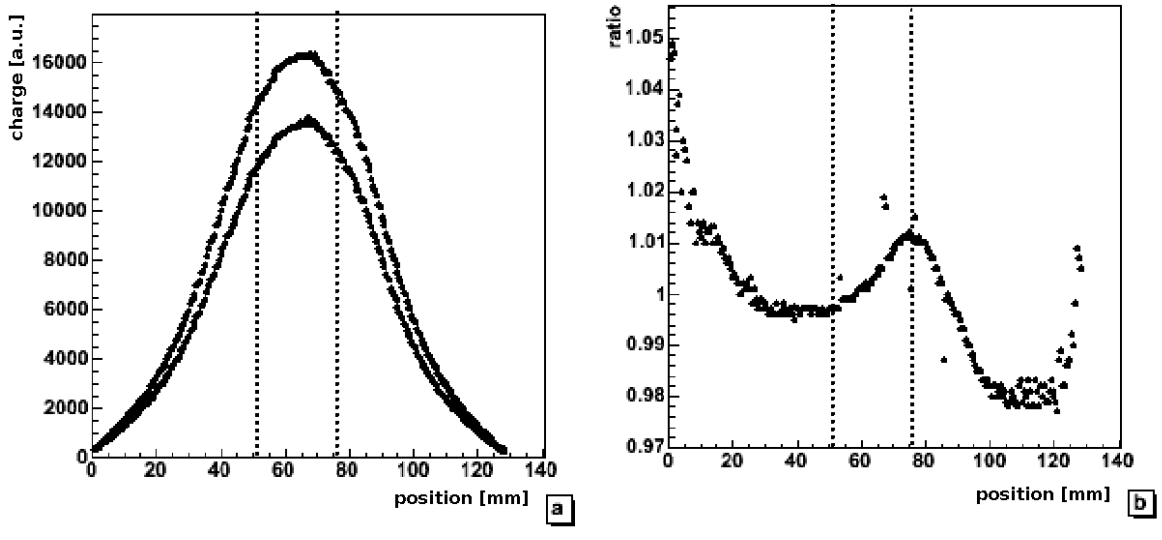

FIG. 9. (a) Horizontal beam projections corresponding to two extreme values of the skewness of Fig.6. (b) Ratio between the two distributions normalized to the same area.

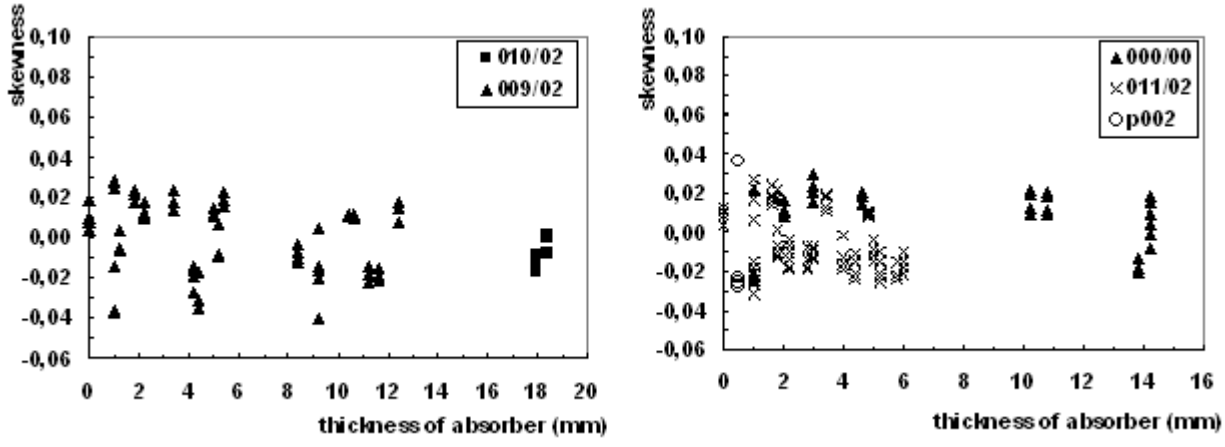

FIG. 10. Skewness of the horizontal beam projection averaged over a single treatment fraction as a function of the thickness of the range shifter (RS). Different symbols correspond to different range modulators.

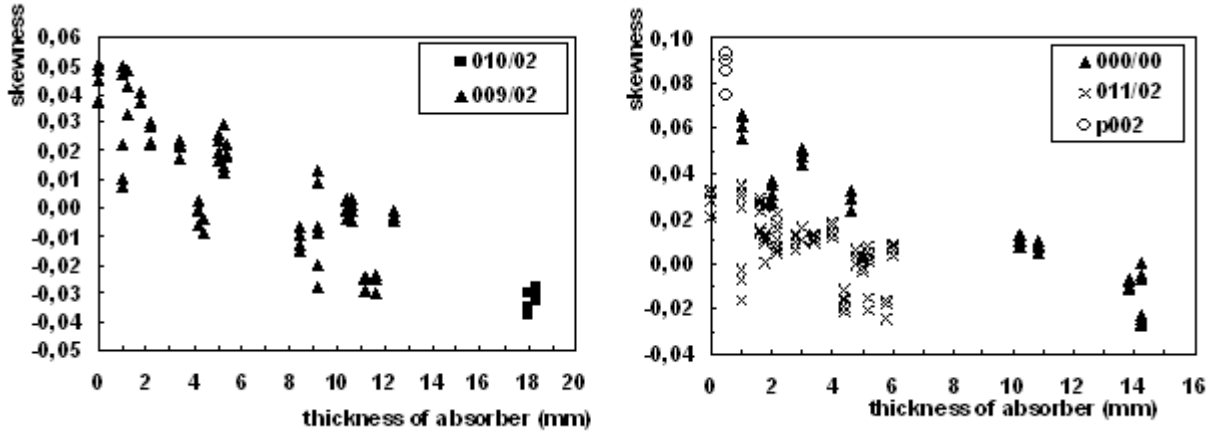

FIG. 11. Skewness of the vertical beam projection averaged over a single treatment fraction as a function of the thickness of the range shifter (RS). Different symbols correspond to different range modulators.

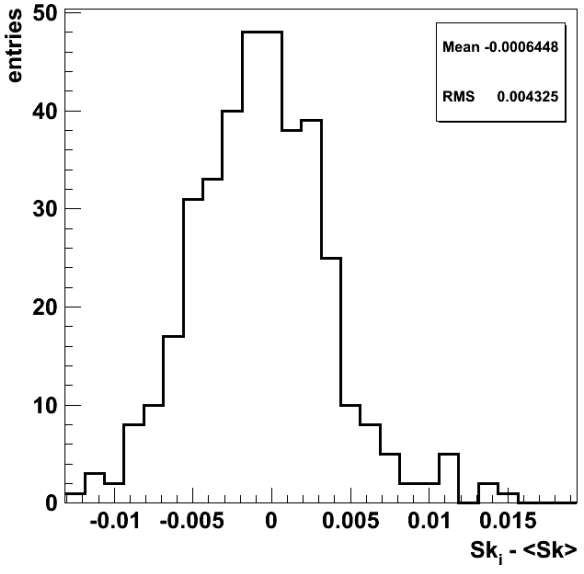

FIG. 12. Distribution of the deviations between the skewness averaged over a fraction and over the whole (4 fractions) treatment.

The mean value of the distribution is -0.0003 and the RMS is 0.0046.